Electronic Supplementary Material (ESI) for Journal of Materials Chemistry C.

Electronic Supplementary Information

A comprehensive structural and microstructural investigation of a new Iron-Telluride nano phase

Kelli Fátima Ulbrich,[a] Federica Bertolotti,[b,c] Norberto Masciocchi,[c,d,*] Antonio Cervellino,[e] Antonietta Guagliardi [c,f] and Carlos Eduardo Maduro de Campos [a,*]

[a] *Departamento de Física, Universidade Federal de Santa Catarina, Campus Trindade, 88 040-900 Florianópolis, Santa Catarina - SC, Brazil. E-mail: carlos.campos@ufsc.br*

[b] *Aarhus Institute of Advanced Studies (AIAS), Aarhus University, Høegh-Guldbergs Gade 6B, 8000 Aarhus C, Denmark.*

[c] *Total Scattering Laboratory (To.Sca.Lab.), Via Valleggio 11, 22100 Como, Italy.*

[d] *Dipartimento di Scienza e Alta Tecnologia, University of Insubria, Via Valleggio 11, 22100 Como, Italy. E-mail: norberto.masciocchi@uninsubria.it*

[e] *Swiss Light Source, Paul Scherrer Institut, 5232 Villigen, Switzerland*

[f] *Istituto di Cristallografia, Consiglio Nazionale delle Ricerche, via Valleggio 11, 22100 Como, Italy*

Materials

Elemental Fe (Sigma-Aldrich 97% purity, 325 mesh) and Te (two batches from Sigma-Aldrich were used, both with 99.997% purity, the one called "old" is granular with 30 mesh and that called "new" is a fine powder with -40 mesh, see Fig S1).

Laboratory X-Ray Powder Diffraction

XRPD experiments were performed on powders of the Fe_xTe materials, deposited in the hollow of silicon zero background sample holder, 0.2 mm deep. Diffraction data were collected on a vertical-scan Panalytical X'Pert Multi-Purpose diffractometer operating in θ:θ mode, equipped with a linear position-sensitive X'Celerator detector, primary and secondary beam Soller slits of 0.04 rad, and Ni-filtered Cu-Kα radiation (λ = 1.5418 Å). Generator settings: 45 kV, 40 mA. High(er) resolution XRPD data of the annealed x = 1.5 sample were collected in the 12-152° 2θ range, with Δ2θ = 0.0334° and used for structure determination of the Fe_5Te_4 phase. In this configuration, a fixed divergent slit of 1/8° aperture, 0.02 rad Soller slits, 2×Ge(220) hybrid W/Si monochromator, providing pure Cu-$K\alpha_1$ radiation (λ = 1.54056 Å), were employed. Using the full crystal structure determination of Fe_5Te_4, discussed in the paper, the Rietveld method was used to assess the amount of the contaminant phases observed at x = 1.0 and x = 1.5.

Structure determination by X-ray powder diffraction

Accurate estimates of the low-angle peak positions of the in-house diffraction data, collected on a vacuum-annealed (500°C) sample, were derived by profile fitting procedures. Subsequently, the SVD indexing algorithm [1] implemented in TOPAS-R [2] provided approximate cell parameters: a = b = 9.40 Å, c = 3.97 Å, with figure of merit = 54.2. [3] Systematic absences indicated the occurrence of an I-centered tetragonal cell. Based on the existence of a few isomorphous systems, retrieved from the 2017 version of the Inorganic Chemistry Structural Database (ICSD), *I4/m* was chosen as probable

space group, with starting coordinates taken from those of the Ti_5Se_4 phase [4] and convergence to the structural model presented below soon reached. Additionally, to avoid any bias in deriving the proposed structural model, a true *ab-initio* procedure was performed, starting, in parallel simulations, from two or three crystallographically independent atoms with relaxed site occupancy factors, freely rattling in the unit cell, following a simulating annealing procedure. Using previously derived experimental factors (background, crystal size, lattice parameters), accurately determined by whole profile structureless refinement, several runs of 100.000 cycles each were completed, all converging to the same crystal structure model, no structural alternatives being found. The structural refinement was carried out by the Rietveld method as follows: the background was modeled by a 4^{th} order polynomial function of the Chebyshev type and a 1/x component for the low angle section, peak profiles were described by the Fundamental Parameters Approach, [5] an isotropic lorentzian broadening of $1/\cos\theta$ dependence. Refinable isotropic thermal factors were individually attributed to all atoms. Tiny peaks attributable to residual nanocrystalline iron were also modeled. Fractional atomic coordinates (reported in Table 1 of the main text) and crystal structure details were deposited within the ICSD [6] (ICSD Code 433719).

Synchrotron Wide Angle X-ray Total Scattering Experiments

Synchrotron WAXTS measurements were performed at the X04SA-MS beamline [7] of the Swiss Light Source (Paul Scherrer Institut, Villigen, CH). Dry powders of nanosized Fe_5Te_4 were loaded inside a 0.5 mm-diameter borosilicate glass capillary of certified composition. The operational beam energy was set at 22 KeV (λ = 0.563829 Å) and accurately determined using a Silicon powder standard (NIST 640d, a_0 = 0.543123(8) nm at 22.5°C). Diffraction data from the sample were collected in the 0.5°-130° 2θ range using a single photon counting silicon microstrip detector (MYTHEN II), [8] together with the X-ray diffraction patterns of the empty glass capillary and of the sample environment, later subtracted from the pattern of the sample. The transmitted beam from the filled capillary was independently measured in order to estimate the sample absorption coefficient, while the computed X-ray attenuation factors from the nominal

glass composition were used for the empty capillary. Angle-dependent intensity corrections were then applied to the raw data, using locally developed routines. [9] The inelastic Compton scattering signal was added as additional model component during the data analysis.

References

[1] A.A. Coelho, Indexing of powder diffraction patterns by iterative use of singular value decomposition, J. Appl. Cryst. 36 (2003) 86-95.

[2] Topas-R, V. 3.0, Bruker AXS, 2007,Karlsruhe, Germany.

[3] The modified Smith & Snyder indexing figure of merit (G. S. Smith and R. L. Snyder, FN: A criterion for rating powder diffraction patterns and evaluating the reliability of powder-pattern indexing), J. Appl. Crystallogr. 12 (1979) 60-65.

[4] M. He, A. Simon, V. Duppel, Ti5Se4: The First Step of Cluster Condensation with Titanium Selenides, Z. Anorg. Allg. Chem. 630(4) (2004) 535-540.

[5] R.W. Cheary, A. Coelho, A Fundamental Parameters Approach to X-ray Line-Profile Fitting, J. Appl. Cryst. 25 (1992) 109-121.

[6] ICSD Database, Version 2017-1, 2017, Fachinformationszentrum Karlsruhe, Germany.

[7] P. R. Willmott, D. Meister, S. J. Leake, M. Lange, A. Bergamaschi, M. Boge, M. Calvi, C. Cancellieri, N. Casati, A. Cervellino, Q. Chen, C. David, U. Flechsig, F. Gozzo, B. Henrich, S. Jaggi-Spielmann, B. Jakob, I. Kalichava, P. Karvinen, J. Krempasky, A. Ludeke, R. Luscher, S. Maag, C. Quitmann, M. L. Reinle-Schmitt, T. Schmidt, B. Schmitt, A. Streun, I. Vartiainen, M. Vitins, X. Wang and R. Wullschleger, *J. Synchrotron Rad.*, 2013, 20, 667-682.

[8] A. Bergamaschi, A. Cervellino, R. Dinapoli, F. Gozzo, B. Henrich, I. Johnson, P. Kraft, A. Mozzanica, B. Schmitt and X. Shi, *J. Synchrotron Rad.*, 2010, 17, 653-668.

[9] A. Cervellino, R. Frison, N. Masciocchi and A. Guagliardi, *Kumar, Challa S.S.R. (Ed.), Springer Verlag*, 2016, Chapter 10, 545-608.

Supplementary Figures

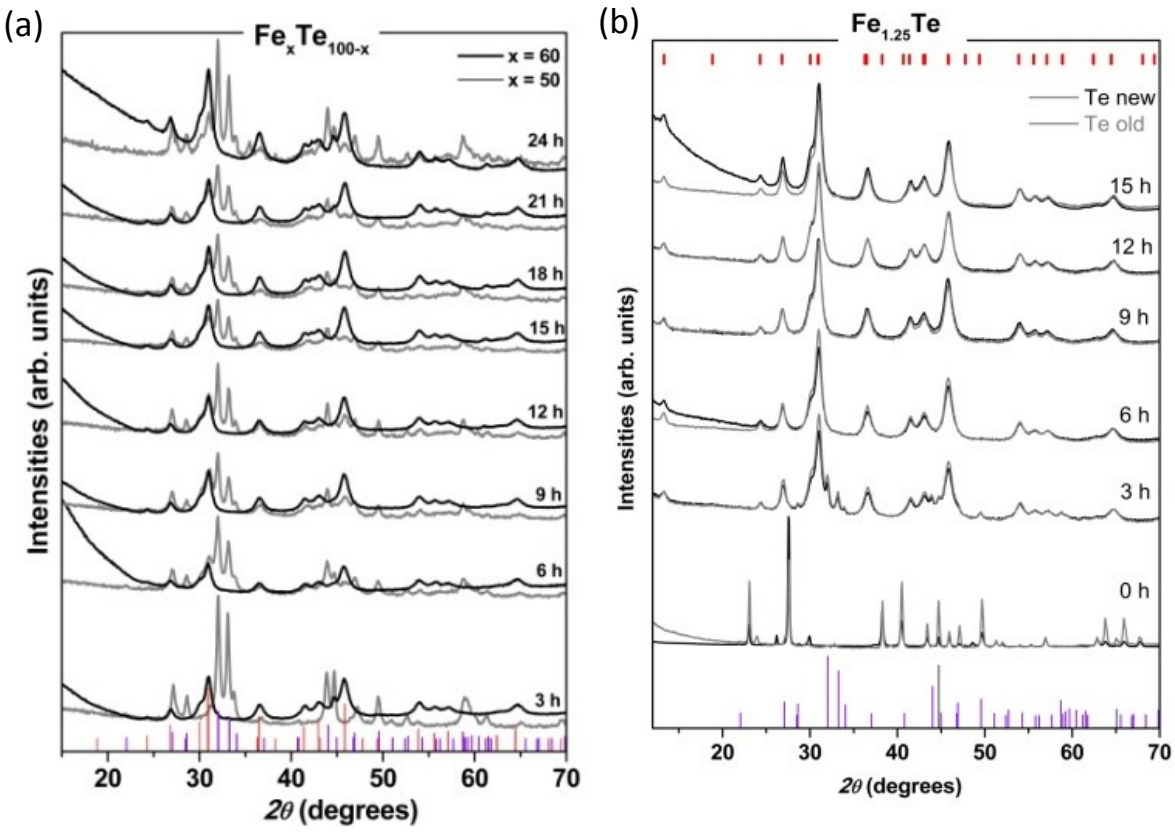

Supplementary Fig. S1 (a) XRD patterns of the $Fe_{1.0}Te$ and $Fe_{1.5}Te$ samples as a function of milling time. (b) XRD patterns of the $Fe_{1.25}Te$ samples (obtained with two different Te batches) as a function of milling time. The red symbols are for representing the peak positions and relative intensities of the Fe_5Te_4 phase and the purple one are for $FeTe_2$.

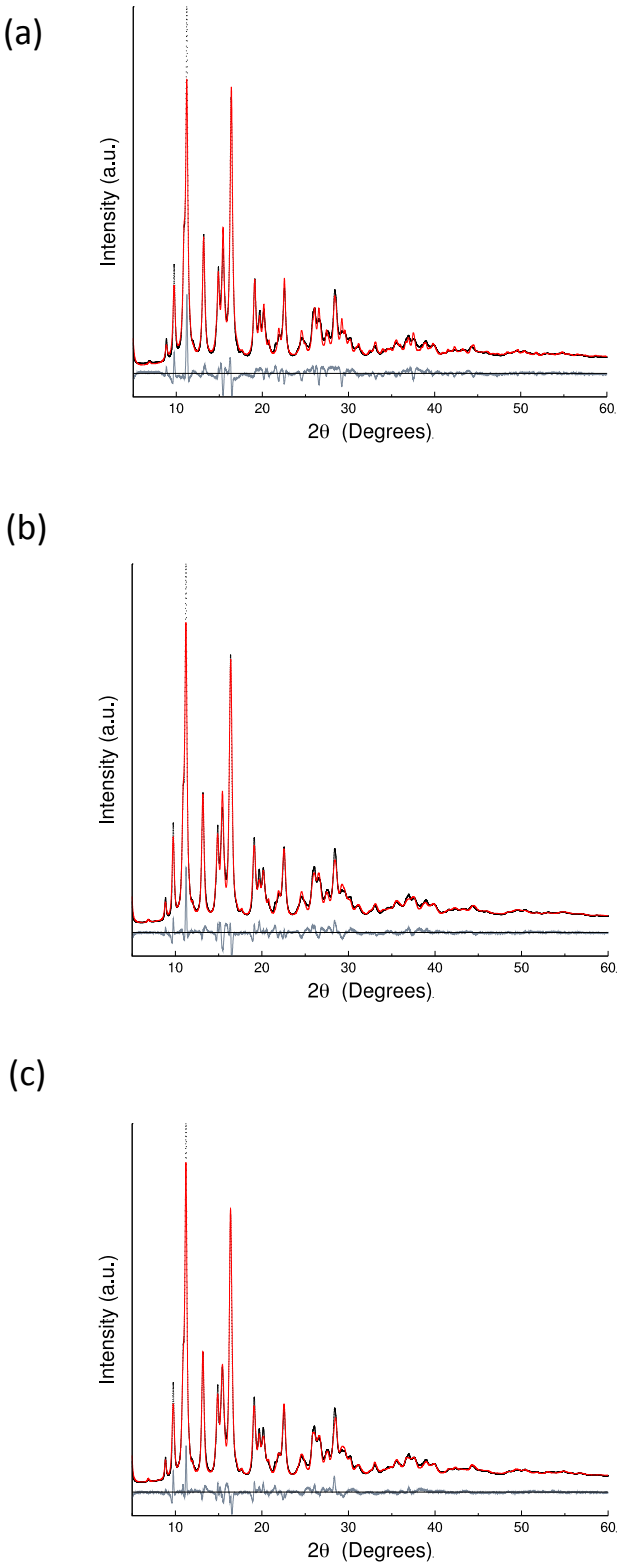

Supplementary Fig. S2. Rietveld refinement plots for synchrotron data of Fe_5Te_4, using an isotropic size model, and different phenomenological models of microstrain: a) zero microstrain (R_{wp} = 8.42); b) isotropic microstrain (R_{wp} = 6.64); c) anisotropic microstrain (by a second order spherical harmonics approximation, and using the conventional tanθ dependence of the peak width of the Gaussian component to peak broadening) (R_{wp} = 6.00).

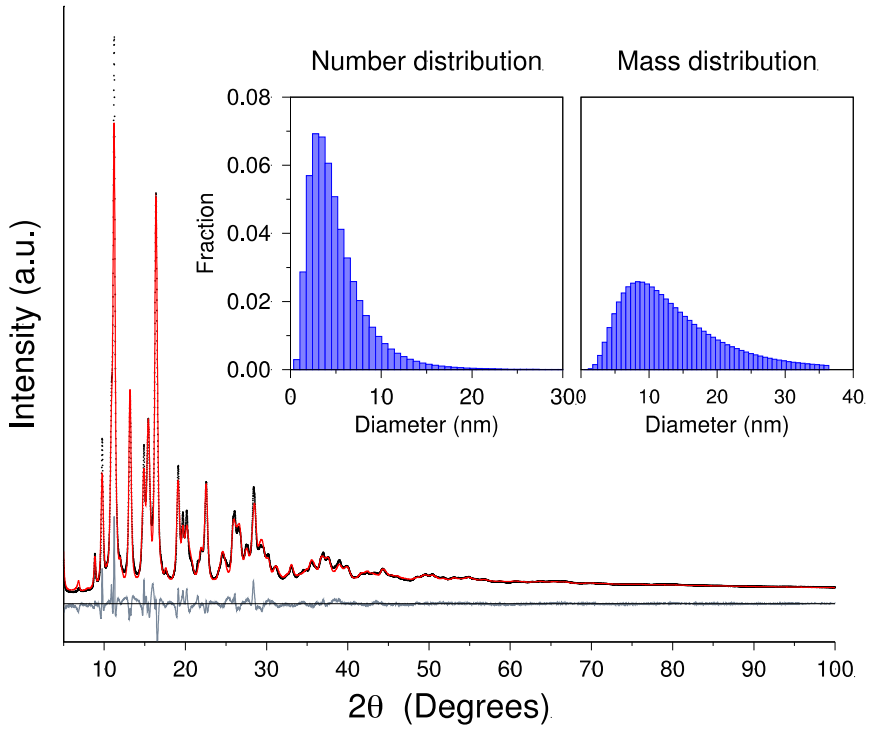

Supplementary Fig. S3. DSE best fit (red trace) obtained using a spherical highly-disperse mono-modal population of Fe_5Te_4 nanocrystals (GoF=14.70). The lognormal number- and mass-based size distributions are reported in the inset, to be compared with the ones shown in Figure 5c of the main text.

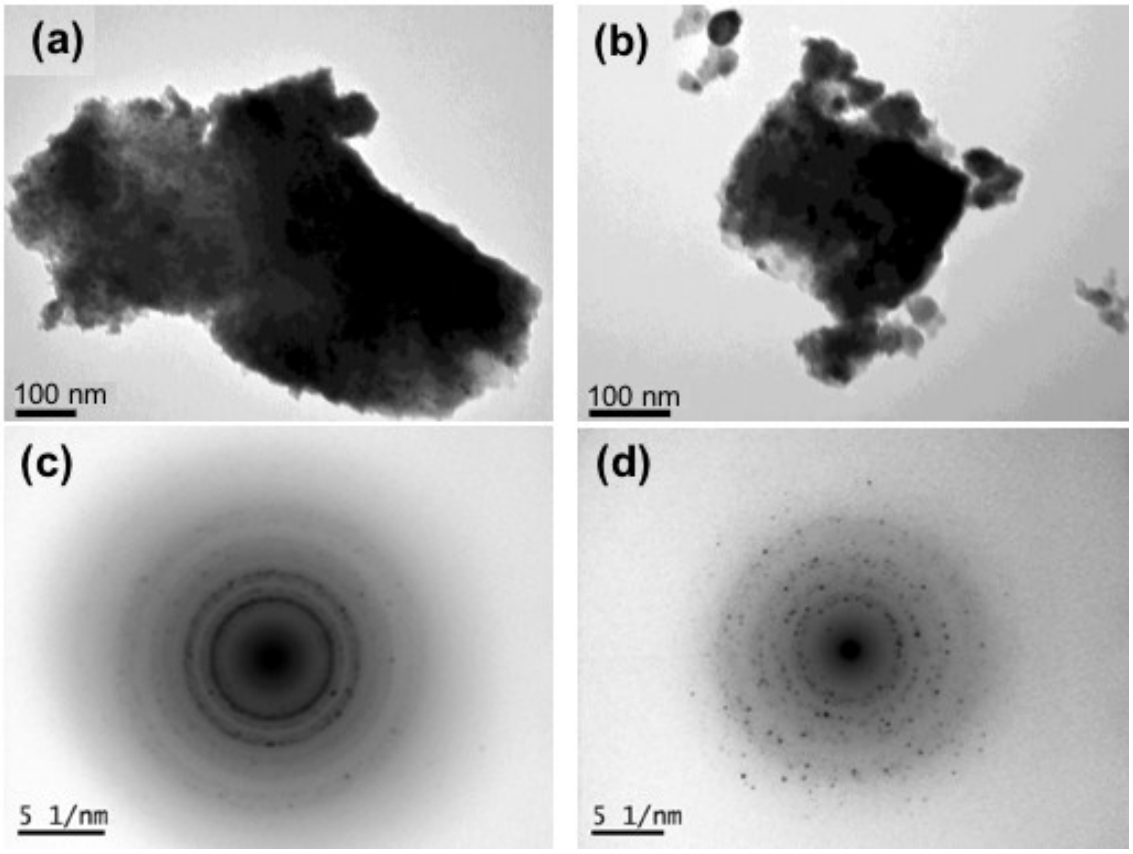

Supplementary Fig. S4. a) and (b): TEM images of as-milled and post-annealed $Fe_{1.5}Te$ samples, respectively, with their SAED plots in (c) and (d).

Supplementary Tables

Supplementary Table 1 Synoptic collection of lattice and structural parameters for all known M_5Q_4 phases, including the ratios of different M-M and M-Q distances. a, c, M_1-M_2, M_2-M_2, M_1-Q, M_2-Q in Å. The dimensionless parameters R_M and R_Q are defined in the text. Bold characters indicate the outliers, as derived for the Fe_5Te_4 phase. All other values have been computed from the structural models deposited within the ICSD database.[6]

M	Q	a	c	a/c	M_1-M_2	M_2-M_2	R_M	M_1-Q	M_2-Q	R_Q
Ti	Te	10.16	3.77	2.69	2.91	3.21	1.103	2.90	2.77	0.955
V	Te	9.81	3.50	2.80	2.70	2.92	1.081	2.87	2.74	0.955
Fe	Te	9.40	3.97	2.37	2.67	2.52	**0.944**	2.69	2.77	**1.030**
Zr	Te	10.76	3.84	2.80	3.08	3.41	1.107	2.90	2.77	0.955
Hf	Te	10.67	3.75	2.85	3.16	3.60	1.139	3.08	2.89	0.938
Nb	Te	10.23	3.71	2.76	2.95	3.24	1.098	2.93	2.82	0.962
Nb	Se	9.87	3.45	2.86	2.74	3.01	1.099	2.82	2.68	0.950
V	Se	9.29	3.42	2.72	2.69	2.95	1.097	2.66	2.63	0.989
V	S	8.99	3.22	2.79	2.58	2.86	1.109	2.57	2.46	0.957

Supplementary Table 2. Rietveld refinement parameters obtained for the three cases listed in Supplementary Fig. 2.

Model	Average crystal size, nm	Microstrain in *ab*, %	Microstrain in *c*, %	R_{wp}, %	R_{Bragg}, %
None	10.5	0	0	8.42	3.86
Isotropic	14.3	0.66	0.66	6.64	3.29
Anisotropic	16.7	0.69	0.28	6.00	2.93